

Supporting Information for:

Effect of coordination anion substitutions on relaxation dynamics of defect dicubane Zn_2Dy_2 tetranuclear clusters

Hongshan Ke,^{,†} Wen Wei,[†] Yongsheng Yang,[†] Jun Zhang^{*,‡}, Yi-Quan Zhang^{*,#}, Gang Xie[†] and Sanping Chen^{*,†}*

[†]Key Laboratory of Synthetic and Natural Functional Molecule Chemistry of Ministry of Education, College of Chemistry and Materials Science, Northwest University, Xi'an 710069, P. R. China. E-mail: hske@nwu.edu.cn; sanpingchen@126.com

[‡]School of Materials and Chemical Engineering, Anhui Jianzhu University, Hefei, 230601, P. R. China. E-mail: zhangjun@ahjzu.edu.cn

[#]Jiangsu Key Laboratory for NSLSCS, School of Physical Science and Technology, Nanjing Normal University, Nanjing 210023, P. R. China. E-mail: zhangyiquan@njnu.edu.cn.

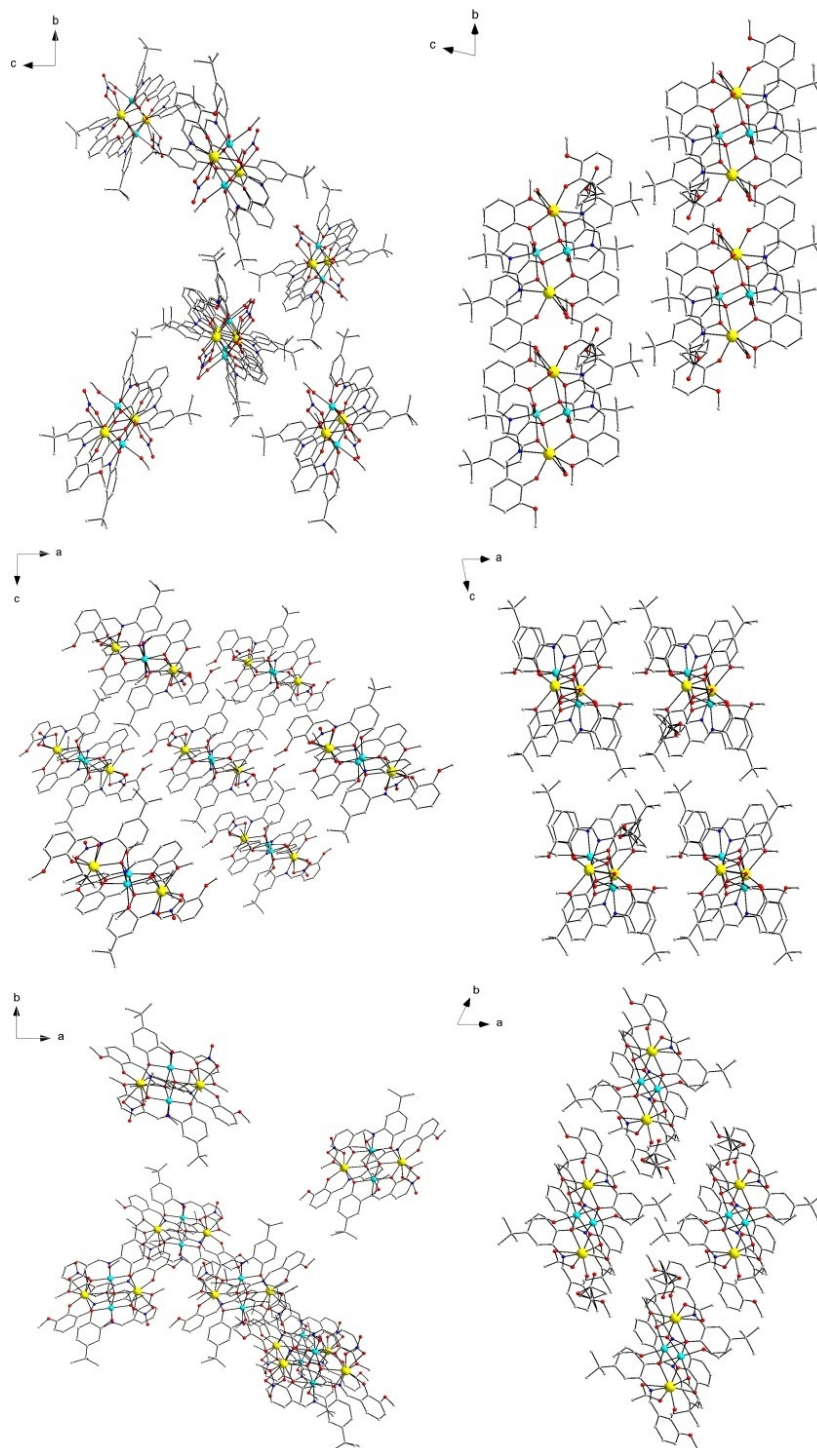


Fig. S1. The crystal packing diagrams for **1** (left) and **2** (right) along the a (top), b (middle) and c (bottom) axis, respectively.

Table S1. Selected bond lengths (Å) and angles (°) for compounds **1** and **2**

1		2	
Bond lengths (Å)			
Zn(1)-N(2)	2.069(5)	Zn(1)-N(2)	2.052(6)
Zn(1)-O(3)	2.064(4)	Zn(1)-O(3)	2.090(5)
Zn(1)-O(3)#1	2.355(4)	Zn(1)-O(3)#2	2.276(5)
Zn(1)-O(5)	2.052(3)	Zn(1)-O(5)	2.073(6)
Zn(1)-O(6)	2.066(4)	Zn(1)-O(6)	2.062(6)
Zn(1)-O(10)	2.177(4)	Zn(1)-O(9)	2.152(5)
Dy(1)-N(1)	2.459(4)	Dy(1)-N(1)	2.446(6)
Dy(1)-O(2)	2.151(4)	Dy(1)-O(2)	2.158(6)
Dy(1)-O(3)	2.377(4)	Dy(1)-O(3)	2.374(5)
Dy(1)-O(4)	2.501(4)	Dy(1)-O(4)	2.490(5)
Dy(1)-O(5)	2.296(4)	Dy(1)-O(5)	2.285(5)
Dy(1)-O(6)#1	2.313(4)	Dy(1)-O(6)#2	2.369(5)
Dy(1)-O(7)	2.512(4)	Dy(1)-O(7)	2.431(5)
Dy(1)-O(8)	2.478(4)	Dy(1)-O(8)	2.448(5)
Zn(1)-Dy(1)	3.4920(8)	Zn(1)-Dy(1)	3.5050(12)
Zn(1)#1-Dy(1)	3.5198(8)	Zn(1)#2-Dy(1)	3.5215(12)
Dy(1)- Dy(1)#1	6.1723(8)	Dy(1)- Dy(1)#2	6.2202(16)
Bond angles (°)			
Zn(1)-O(3)-Dy(1)	103.47(15)	Zn(1)-O(3)-Dy(1)	103.3(2)
Zn(1)#1-O(3)-Dy(1)	96.14(14)	Zn(1)#2-O(3)-Dy(1)	98.4(2)
Zn(1)-O(5)-Dy(1)	106.73(14)	Zn(1)-O(5)-Dy(1)	107.0(2)
Zn(1)-O(6)-Dy(1)#1	106.83(16)	Zn(1)-O(6)-Dy(1)#2	105.0(2)
Zn(1)-O(3)-Zn(1)#1	97.46(16)	Zn(1)-O(3)-Zn(1)#2	96.8(2)

Symmetry transformations used to generate equivalent atoms: **1** and **2** #1
-x, 1-y, -z, #2 2-x, 1-y, 2-z.

Table S2. SHAPE¹ analysis of compounds **1** and **2**

Configuration	ABOXIY, 1	ABOXIY, 2
Octagon(D _{8h})	32.666	33.346
Heptagonal pyramid(C _{7v})	22.305	21.685
Hexagonal bipyramid(D _{6h})	15.200	15.684
Cube(O _h)	10.383	11.496
Square antiprism(D _{4d})	2.971	3.286
Triangular dodecahedron(D_{2d})	2.656	2.665
Johnson gyrobifastigium J26(D _{2d})	13.331	13.790
Johnson elongated triangular bipyramid J14(D _{3h})	26.913	26.274
Biaugmented trigonal prism J50(C _{2v})	2.867	2.969
Biaugmented trigonal prism(C_{2v})	2.430	2.491
Snub diphenoid J84(D _{2d})	4.488	4.917
Triakis tetrahedron(T _d)	11.074	12.157
Elongated trigonal bipyramid(D _{3h})	23.242	23.476

Table S3. Fitted exchange coupling constant J_{exch} , the calculated dipole-dipole interaction J_{dip} and the total J between Dy^{III} ions in complexes **1** and **2** (cm⁻¹). The intermolecular interactions zJ' of complexes **1** and **2** were fitted to 0.00 cm⁻¹.

	1	2
J_{exch}	-0.25	-0.25
J_{dip}	0.66	0.62
J	0.41	0.37

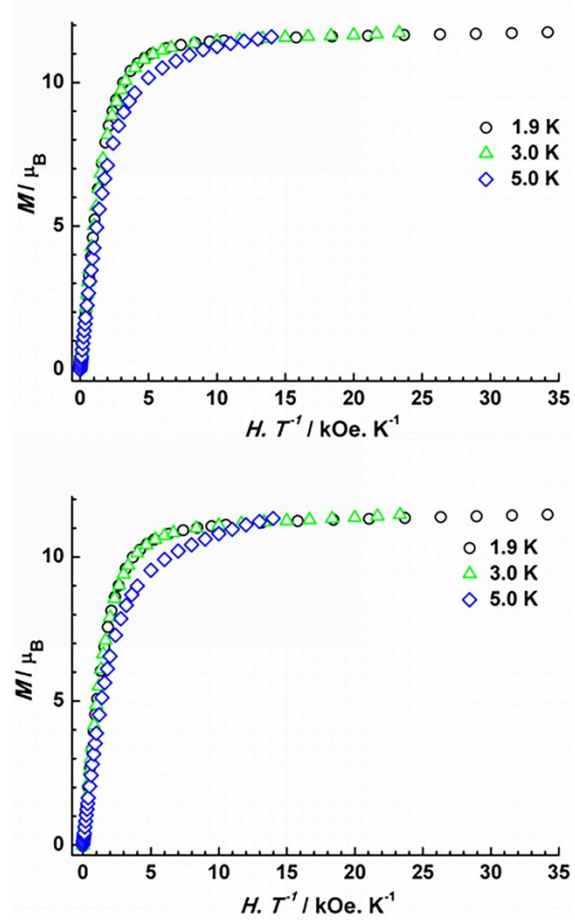


Fig. S2. Field dependence of the reduced magnetization for **1** (top) and **2** (bottom) at 1.9, 3 and 5 K.

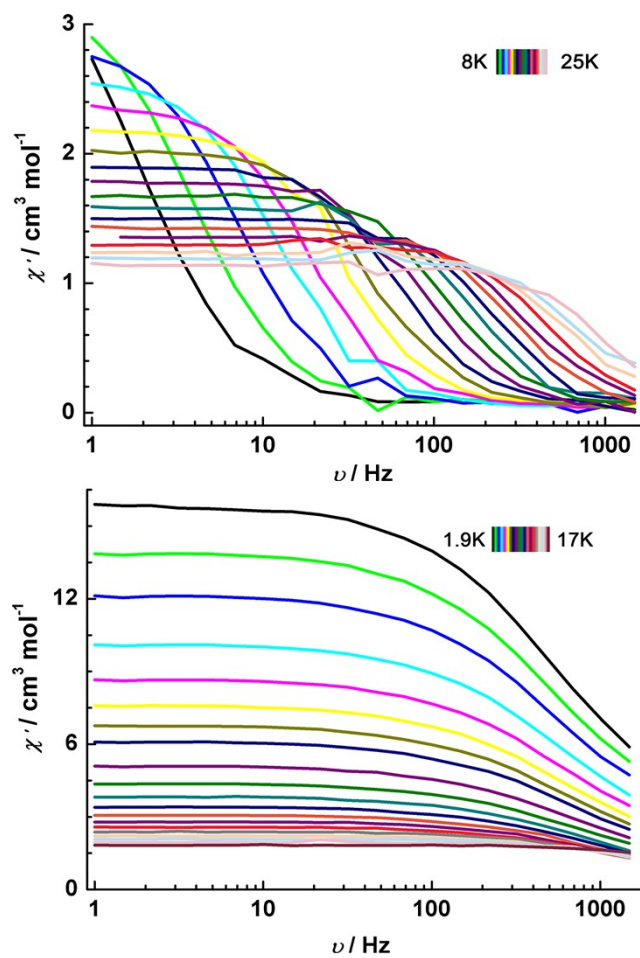


Fig. S3. Frequency dependence of in-phase (χ_M') components of the ac magnetic susceptibility signals for **1**(top) and **2** (bottom) under zero applied dc field and an oscillating field of 3.5 Oe.

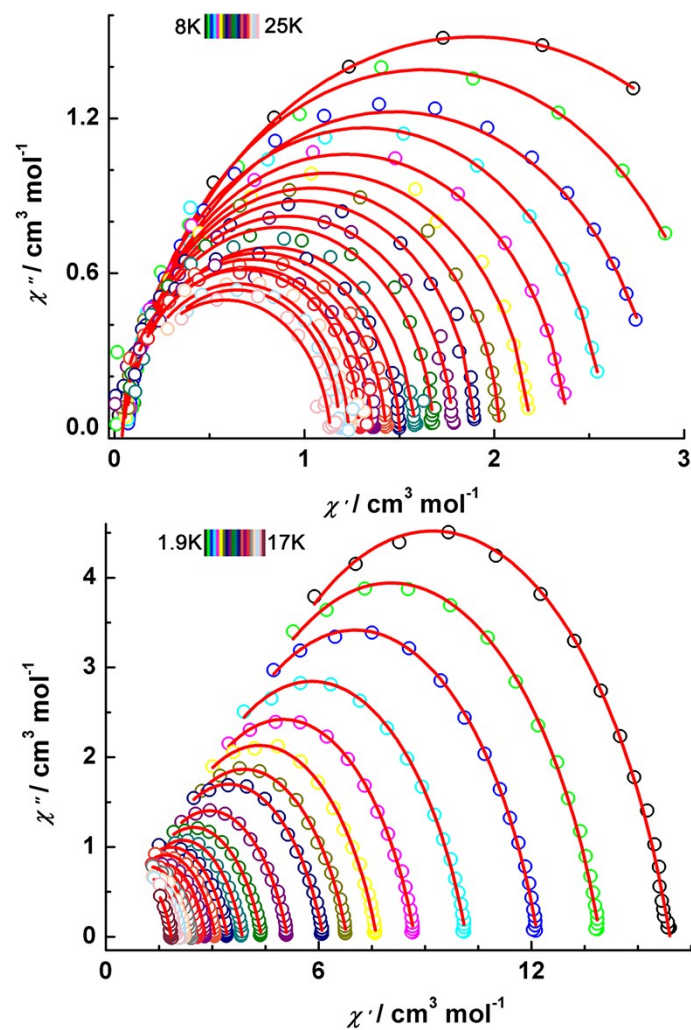


Fig. S4. Cole-Cole² (Argand) plots for ac susceptibility collected at zero applied dc field for **1** (top) and **2** (bottom). Solid curves represent theoretical calculations on the basis of the generalized Debye model.³

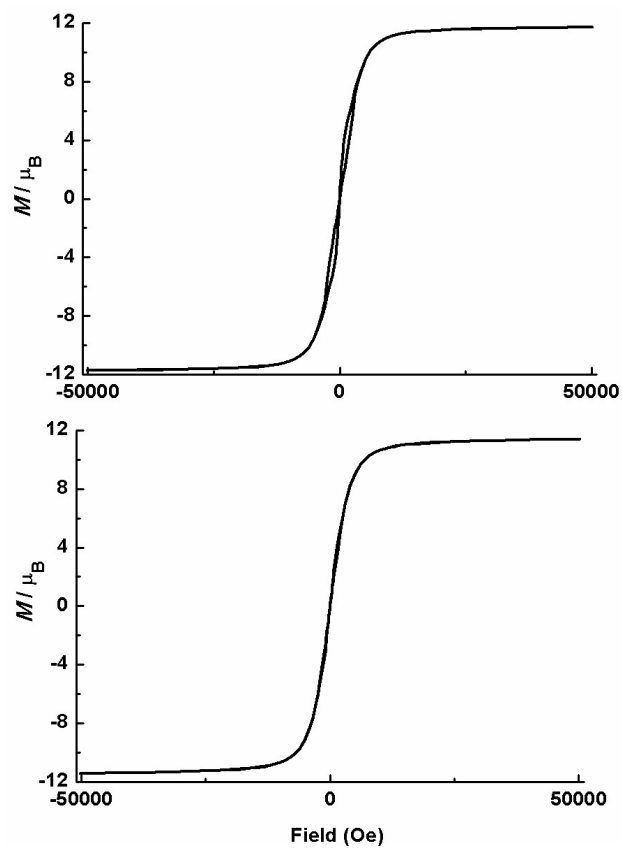


Figure S5. Magnetization versus applied direct-current field scan measured at 1.9 K for **1** (top) and **2** (bottom) while sweeping the field from 5 to -5 T.

Table S4. χ_S , χ_T , τ and α values of **1** and **2** estimated by theoretical calculations on the basis of the generalized Debye model³

1								
T/K	8	9	10	11	12	13	14	15
$\chi_S/\text{cm}^3 \text{ mol}^{-1}$	0.05	0.05	0.07	0.05	0.05	0.06	0.05	0.03
$\chi_T/\text{cm}^3 \text{ mol}^{-1}$	3.72	3.21	2.86	2.59	2.38	2.18	2.03	1.91
α	0.12	0.08	0.07	0.06	0.05	0.04	0.04	0.05
τ/s	0.08248	0.04049	0.02249	0.01278	0.00831	0.00518	0.00361	0.00248
T/K	16	17	18	19	20	21	22	23
$\chi_S/\text{cm}^3 \text{ mol}^{-1}$	0.04	0.05	0.07	0.05	0.01	0.04	0.03	0.07
$\chi_T/\text{cm}^3 \text{ mol}^{-1}$	1.79	1.68	1.57	1.50	1.43	1.36	1.31	1.25
α	0.04	0.03	0.02	0.03	0.06	0.04	0.03	0.02
τ/s	0.00182	0.0013	0.00098	0.000745	0.00056	0.00043	0.000342	0.000273
T/K	24	25						
$\chi_S/\text{cm}^3 \text{ mol}^{-1}$	0.08	0.11						
$\chi_T/\text{cm}^3 \text{ mol}^{-1}$	1.20	1.14						
α	0.03	0.01						
τ/s	0.00022	0.000187						
2								
T/K	1.9	2.2	2.5	3	3.5	4	4.5	5
$\chi_S/\text{cm}^3 \text{ mol}^{-1}$	2.43	2.06	1.82	1.43	1.24	1.02	1.02	0.80
$\chi_T/\text{cm}^3 \text{ mol}^{-1}$	15.92	13.96	12.19	10.17	8.72	7.64	6.79	6.13
α	0.25	0.26	0.26	0.26	0.27	0.27	0.27	0.28
τ/s	0.000294	0.000285	0.000278	0.000264	0.000255	0.000246	0.000251	0.000232
T/K	6	7	8	9	10	11	12	13
$\chi_S/\text{cm}^3 \text{ mol}^{-1}$	0.72	0.52	0.54	0.24	0.26	0.43	0.20	0.12
$\chi_T/\text{cm}^3 \text{ mol}^{-1}$	5.12	4.40	3.85	3.43	3.09	2.81	2.59	2.39
α	0.28	0.29	0.26	0.29	0.27	0.24	0.26	0.24
τ/s	0.000254	0.000201	0.000208	0.000162	0.000157	0.000161	0.000124	0.000097
								1
T/K	14	15	16	17				
$\chi_S/\text{cm}^3 \text{ mol}^{-1}$	0.30	0.40	0.14	0.44				
$\chi_T/\text{cm}^3 \text{ mol}^{-1}$	2.22	2.08	1.96	1.83				
α	0.21	0.17	0.20	0.13				
τ/s	0.000094	0.000085	0.000045	0.000043				
	4	5	1	8				

Table S5. χ_S , χ_T , and α parameters of **1** and **2** derived from Cole-Cole fitting²

1								
T/K	8	9	10	11	12	13	14	15
$\chi_T/\text{cm}^3 \text{ mol}^{-1}$	3.728	3.188	2.88	2.579	2.383	2.187	2.027	1.897
$\chi_S/\text{cm}^3 \text{ mol}^{-1}$	0.057	0.0748	0.0683	0.06	0.053	0.0512	0.052	0.0638
α	0.121	0.072	0.0866	0.0502	0.0594	0.0493	0.0381	0.025
T/K	16	17	18	19	20	21	22	23
$\chi_T/\text{cm}^3 \text{ mol}^{-1}$	1.782	1.677	1.581	1.500	1.428	1.360	1.295	1.222
$\chi_S/\text{cm}^3 \text{ mol}^{-1}$	0.0405	0.0542	0.0621	0.0393	0.0137	0.0188	0.041	0.2
α	0.0388	0.0263	0.0511	0.042	0.0498	0.060	0.023	0.01
T/K	24	25						
$\chi_T/\text{cm}^3 \text{ mol}^{-1}$	1.184	1.131						
$\chi_S/\text{cm}^3 \text{ mol}^{-1}$	0.102	0.053						
α	0.0068	0.052						
2								
T/K	1.9	2.2	2.5	3	3.5	4	4.5	5
$\chi_T/\text{cm}^3 \text{ mol}^{-1}$	15.901	13.938	12.178	10.160	8.706	7.632	6.793	6.128
$\chi_S/\text{cm}^3 \text{ mol}^{-1}$	2.520	2.131	1.871	1.450	1.292	1.023	1.017	0.798
α	0.243	0.250	0.255	0.263	0.263	0.271	0.270	0.277
T/K	6	7	8	9	10	11	12	13
$\chi_T/\text{cm}^3 \text{ mol}^{-1}$	5.117	4.389	3.847	3.423	3.083	2.807	2.585	2.392
$\chi_S/\text{cm}^3 \text{ mol}^{-1}$	0.736	0.571	0.510	0.259	0.292	0.449	0.228	0.0752
α	0.274	0.276	0.272	0.284	0.264	0.234	0.250	0.245
T/K	14	15	16	17				
$\chi_T/\text{cm}^3 \text{ mol}^{-1}$	2.213	2.079	1.954	1.839				
$\chi_S/\text{cm}^3 \text{ mol}^{-1}$	0.476	0.277	0.234	0.201				
α	0.171	0.199	0.228	0.214				

Table S6. Calculated energy levels (cm^{-1}), \mathbf{g} (g_x, g_y, g_z) tensors and m_J values of the lowest eight Kramers doublets (KDs) of individual Dy^{III} fragments of **1** and **2**

KDs	1			2		
	E/cm^{-1}	\mathbf{g}	m_J	E/cm^{-1}	\mathbf{g}	m_J
1	0.0	0.005	$\pm 15/2$	0.0	0.015	$\pm 15/2$
		0.006			0.021	
		19.676			19.616	
2	220.3	0.124	$\pm 13/2$	184.0	0.132	$\pm 13/2$
		0.179			0.261	
		16.825			16.516	
3	367.5	2.323	$\pm 9/2$	267.3	1.345	$\pm 3/2$
		3.925			1.873	
		14.541			17.550	
4	427.0	8.356	$\pm 11/2$	333.6	2.003	$\pm 11/2$
		5.495			4.358	
		1.243			10.496	
5	505.0	1.260	$\pm 5/2$	373.4	0.618	$\pm 7/2$
		3.309			4.698	
		16.382			12.331	
6	538.1	2.536	$\pm 3/2$	438.9	3.328	$\pm 5/2$
		4.762			5.384	
		10.570			11.556	
7	617.3	0.594	$\pm 1/2$	503.1	0.409	$\pm 1/2$
		1.015			0.582	
		16.228			16.749	
8	682.3	0.115	$\pm 7/2$	601.7	0.029	$\pm 9/2$
		0.167			0.055	
		18.945			19.171	

Table S7. Wave functions with definite projection of the total moment $|m_J\rangle$ for the lowest two Kramers doublets (KDs) of individual Dy^{III} fragments for **1** and **2**

	E/cm^{-1}	wave functions
1	0.0	97% $ \pm 15/2\rangle$
	220.3	91% $ \pm 13/2\rangle$ +4% $ \pm 9/2\rangle$
2	0.0	96% $ \pm 15/2\rangle$
	184.0	89% $ \pm 13/2\rangle$ +4% $ \pm 9/2\rangle$ +3% $ \pm 7/2\rangle$

Table S8. Exchange energies (cm^{-1}) and main values of the g_z for the lowest two exchange doublets of complexes **1** and **2**

	1		2	
	E/cm^{-1}	g_z	E/cm^{-1}	g_z
1	0.0	39.353	0.0	39.233
2	0.2	0.000	0.2	0.000

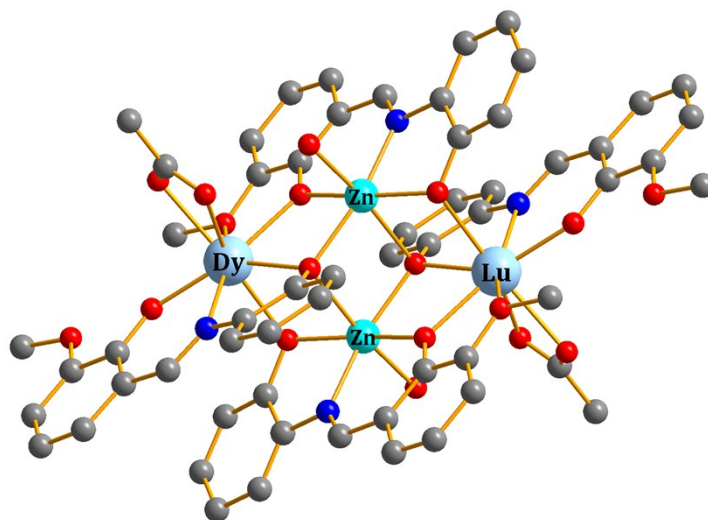


Fig. S6. Calculated model structure of individual Dy^{III} fragment of **2**; H atoms are omitted.

References

- 1 D. Casanova, M. Llunell, P. Alemany and S. Alvarez, *Chem. -Eur. J.*, 2005, **11**, 1479.
- 2 K. S. Cole and R. H. Cole, *J. Chem. Phys.*, 1941, **9**, 341.
- 3 S. M. J. Aubin, Z. Sun, L. Pardi, J. Krzystek, K. Folting, L.-C. Brunel, A. L. Rheingold, G. Christou and D. N. Hendrickson, *Inorg. Chem.*, 1999, **38**, 5329.